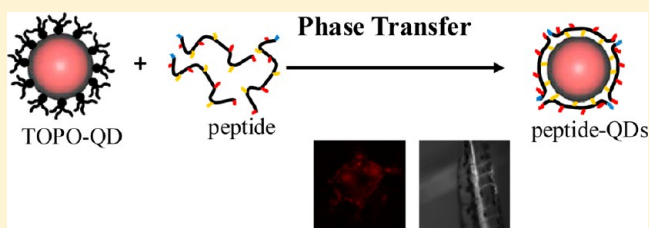


# Stable, Compact, Bright Biofunctional Quantum Dots with Improved Peptide Coating

Jianmin Xu,<sup>†</sup> Piotr Ruchala,<sup>‡</sup> Yuval Ebenstein,<sup>†</sup> J. Jack Li,<sup>†</sup> and Shimon Weiss<sup>\*,†,§,||</sup><sup>†</sup>Department of Chemistry & Biochemistry, <sup>‡</sup>David Geffen School of Medicine, <sup>§</sup>Department of Physiology, and <sup>||</sup>California NanoSystems Institute, University of California at Los Angeles, Los Angeles, California 90095, United States

## S Supporting Information

**ABSTRACT:** We developed a new peptide, natural phytochelatin (PC), which tightly binds to CdSe/ZnS quantum dots (QDs) surfaces and renders them water-soluble. Coating QDs with this flexible and all-hydrophilic peptide offers high colloidal stability, adds only 0.8–0.9 nm to the radius of the particles (as compared to their original inorganic radius), preserves very high quantum yield (QY) in water, and affords facile bioconjugation with various functional groups. We demonstrate specific targeting (with minimal nonspecific binding) of such fluorescein-conjugated QDs to ScFv-fused mouse prion protein expressed in live N2A cells. We also demonstrated homogeneous in vivo biodistribution with no significant toxicity in live zebrafish.



## INTRODUCTION

Fluorescent quantum dots (QDs) have been widely adopted for various bioimaging applications due to their unique photo-physical properties.<sup>1–4</sup> Since high quality QDs are often synthesized in organic solvents,<sup>5–7</sup> an additional (coating) step is required to render them water-soluble before they can be used in such applications. Ideally, this additional step should maintain their small size, colloidal stability, and high quantum yield (QY). In addition, this step should allow for a facile and efficient conjugation of biomolecules of interest to the QDs' surface. Several coating strategies have been developed, roughly divided into two main categories: (i) encapsulation with, for example, amphiphilic polymers<sup>8,9</sup> or phospholipids<sup>10</sup> and (ii) ligand exchange.<sup>11–13</sup> Encapsulation usually yields higher QY QDs (higher than achieved by ligand exchange methods) because it keeps the original surfactant molecules on the QDs' surface, but at the expense of a larger hydrodynamic radius and sometimes colloidal stability.<sup>14</sup> In vivo and tissue-culture molecular imaging applications call for the smallest QD size possible.<sup>15–17</sup> The ligand exchange method, and in particular ligand exchange with small thiolated molecules indeed offers a very thin biocompatible coat, but at the expense of compromised colloidal stability and reduced QY.<sup>18</sup> To address colloidal stability, Mattoussi et al. developed dihydrolipoic acid (DHLLA) bidentate thiol ligands.<sup>12</sup> Yet, DHLLA coated QDs had poor solubility at low pH (below 7; deprotonation of the carboxyl group is needed in order to increase the surface density of COO<sup>−</sup> groups which in turn increases water solubility).<sup>12</sup> The same group also developed coating based on a DHLLA-poly(ethylene glycol) (DHLLA-PEG) derivative which broadened the pH stability window and allowed to tune end-group function and overall particle charge by appending various end groups to the PEG.<sup>19–23</sup> Despite these achieve-

ments, some concerns about the long-term stability of the DHLLA-PEG coating have been raised.<sup>24</sup>

Previously, we reported a ligand exchange approach which is based on phytochelatin-related  $\alpha$ -peptide ligands ("peptide coating").<sup>25–28</sup> These peptides contained multiple cysteines interspaced by hydrophobic residues and were anchored to Zn or Cd ions on the QD surface via the cysteines' thiol groups. The  $\alpha$ -peptide coating provided the QDs with excellent colloidal properties and allowed to modulate their charge, solubility, and functionality via the peptide sequence itself. However, a relatively large and costly amount and difficult-to-synthesize amphiphilic peptide ligands were required to carry out an efficient ligand exchange reaction, and the QY was significantly reduced after the exchange.<sup>29</sup> Therefore, there is still quite a bit of room for improving this approach.

The peptide coating approach was motivated and inspired by the naturally evolved, cysteine-rich peptides called phytochelatins ( $\gamma$ EC)<sub>n</sub>G ( $n = 2–6$ ) and their monomer glutathione (GSH)  $\gamma$ ECG counterparts,<sup>30</sup> which are synthesized by some plants, yeast, and bacteria strains for chelating and detoxifying heavy metal ions (such as Cd<sup>2+</sup>) when present in the environment. These  $\gamma$  structure peptides tightly bind to CdS, ZnS, and CdTe QDs.<sup>31–36</sup> Recently, several groups have used GSH for core shell QDs ligand exchange and have demonstrated improved photophysical properties.<sup>37,38</sup>

In this report, we demonstrate the improved properties and enhanced utility of QDs coated with all-hydrophilic, cysteine-rich,  $\gamma$  structure phytochelatin peptides ( $\gamma$ PC). We demonstrate a QD product which has high colloidal stability, small size, high

Received: June 29, 2012

Revised: August 16, 2012

Published: August 17, 2012

QY, facile bioconjugation, and improved immunocytochemistry and in vivo biodistribution attributes.

## MATERIALS AND METHODS

**Chemicals.** QDs602 ( $\lambda_{\text{em}} = 602$ ) were purchased from Evident Technologies (Ebioscience, San Diego, CA). QDs545 ( $\lambda_{\text{em}} = 545$ ) were synthesized in-house using a published method.<sup>7</sup> Fluorescein-PEG NHS ester (FL-PEG-SVA) and PEG NHS ester (mPEG-SVA) were purchased from Laysan Bio Inc. The peptide GSESGGSESGF(CCF)<sub>3</sub> was purchased from New England Peptide.

**Synthesis of Peptides.** Gamma phytochelatin peptides ( $\gamma$ PC) were purchased from Science Peptide (Shanghai, China) or synthesized in-house by the standard F-moc solid-phase peptide synthesis (SPPS) method. Alpha phytochelatin peptides ( $\alpha$ PC) were also synthesized in-house by SPPS. The identity and purity (>90%) of the peptides were confirmed by mass spectrometry and reversed-phase HPLC (data shown in Supporting Information).

**Peptide Coating.** Coating with a natural  $\alpha$ -phytochelatin-like amphiphilic peptide GSESGGSESGF(CCF)<sub>3</sub>, denoted herein ampPC, was done according to the published protocol.<sup>26,27</sup> A modified coating protocol was used for all other peptides or amino acid monomers: (i) CdSe/ZnS QDs were precipitated by acetone and redissolved in pyridine to a final concentration of  $\sim 1 \mu\text{M}$ ; (ii) an excess of peptides (>6000 $\times$ , typically 4 mg in 50  $\mu\text{L}$  DI water were mixed with 450  $\mu\text{L}$  QDs pyridine solution; (iii) surfactant exchange was triggered by increasing the pH of the mixture (to about pH 10) with addition of 12  $\mu\text{L}$  of tetramethylammonium hydroxide (TMAOH) 25% (w/v) in methanol; (iv) the mixture was quickly vortexed and centrifuged; (v) the pellet was redispersed in DI water; (vi) redispersed QDs were dialyzed against PBS buffer (50 mM NaCl, 10 mM Na<sub>2</sub>HPO<sub>4</sub>, pH 7.2) using a 20 K MWCO Slide-A-Lyzer Mini Dialysis Units (Pierce, Rockford, IL) to remove unbound peptides.

**Chromatographic and Electrophoresis Techniques.** Size exclusion gel chromatography was performed on an Agilent 1100 series liquid chromatography system with coupled G4000SWxL columns (Tosoh, Montgomeryville, PA) using a PBS pH 7.2 mobile phase at a flow rate 0.5 mL/min. Absorbance and fluorescence emission were acquired during the separation.

Gel electrophoresis was performed on 1% agarose gel in 0.5  $\times$  TBE buffer for 1 h at 120 V. The fluorescent bands were detected on a FX fluorescence gel scanner (Biorad, Hercules, CA) with a 488 nm laser excitation and the appropriate emission filter (e.g. 550 long pass for 602 nm QDs).

**Dynamic Light Scattering (DLS).** The mean hydrodynamic diameters were obtained using the 90Plus/Bi-Mas laser scattering system (Brookhaven Instruments Corp.). All samples were centrifuged at a maximum speed of 15 000 rpm for 5 min before measurements. The DLS measurements were performed at an angle of 90° and 25 °C. Each measurement constituted an average of 20 runs.

**Photophysical Characterization.** As-synthesized, organic phase QDs were precipitated by acetone and redispersed in hexane for spectroscopic measurements. Peptide-coated QDs were kept in PBS buffer for spectroscopic measurements. UV-vis absorption spectra were acquired on a Perkin-Elmer lambda 25 UV-vis spectrometer (Perkin-Elmer, Shelton, CT). Fluorescence spectra were acquired on a QM-6SE PTI fluorescence spectrometer with excitation at 420 nm (PTI,

Brimingham, NJ). Both of the excitation and emission slit widths were set at 5 nm.

**Transmission Electron Microscopy.** TEM imaging was performed on a 300 kV high-resolution Titan S/TEM microscope (FEI, Hillsboro, OR). After acetone precipitation, QDs were redispersed in toluene and deposited on ultrathin carbon coated copper grids 400 mesh (Ted Pella, Redding, CA).

**Bioconjugation.** Streptavidins (SAV) were conjugated to  $\gamma$ PC3-602 QDs via carbodiimide using the following protocol: (i) as-prepared  $\gamma$ PC3-602 PBS suspension was buffer exchanged to 0.1 M MES pH 5 by Zeba 20 K Molecular weight cutoff (MWCO) spin column (Pierce, IL), yielding a 2  $\mu\text{M}$  concentration; (ii) a large excess (>3000 $\times$ ) of fresh 1-ethyl-3-[3-dimethylaminopropyl]carbodiimide hydrochloride (EDC) and *N*-hydroxysulfosuccinimide (sulfo-NHS) solutions was added to the QDs suspension; (iii) the solution was shaken for 20 min; (iv) the mixture was eluted by PBS equilibrated zeba spin column to remove the free EDC and sulfo-NHS and transferred to 0.1 M PBS pH 7.4 buffer. Alternatively, step (iv) could be replaced by just adding a 2-mercaptoethanol solution to quench the free EDC and adjusting the pH above 7 with NaOH solution; (v) activated  $\gamma$ PC3-602 QDs were mixed with 70  $\mu\text{L}$  of 10 mg/mL SAV (40 folds) for 4 h at room temperature; (vi) the reaction was quenched by mPEG-amine (550 MW, Laysan Biotech, Arab, AL) solution; (vii) the product was purified by 100K MWCO centrifugal ultrafiltration unit using >6 times buffer (0.1 M PBS pH 7.4) exchanges.

Small molecules (fluorescein) were conjugated to amine groups on the QDs coating via another strategy. FL-PEG-SVA and mPEG-SVA were mixed with molar ratios of 1:9 and 4:6, respectively. Excess FL-PEG-SVA/mPEG-SVA were mixed with peptides for 1 h, and the reaction was then quenched by hydroxylamine for 30 min. The modified peptides were used to coat QDs using the same procedure as described above. Fluorescein coated QDs (named as FL-QDs) were then dialysis against 4 L of PBS pH 7.4 buffer overnight, followed by a purification step using zeba spin column.

**Live Cell Imaging.** A single-chain variable fragment antibody (scFv) against fluorescein (4M5.3 scFv)<sup>39</sup> was fused to the N-terminus of the full length mouse prion protein (PrP) bearing epitope and expressed in mouse neuroblastoma cell line N2A.<sup>40</sup> The cells were grown in high glucose DMEM containing 10% fetal bovine serum. QDs were diluted into the cell medium to a final concentration of 2 nM and incubated for 30 min at room temperature. The cells were then washed by fresh medium 3 times and put in fresh medium for imaging (using a Nikon ECLIPSE Ti with 60 $\times$  oil objective).

**In Vivo Zebrafish Imaging.** Three days post fertilization (dpf) zebrafish embryos were anesthetized in tricaine medium and placed onto a precasted agarose mold. A glass capillary was filled with 1  $\mu\text{M}$  QDs suspension and connected to a MPPI-2 pressure injector system (ASI, Eugene, OR). The capillary was inserted into the beating heart of the embryos, and 2–3 microinjection pulses released QDs suspension into the heart chamber. The injected embryos were immediately observed using a Leica SP1 Upright fluorescence microscope (Leica Microsystems GmbH, Wetzlar, Germany).

## EXPERIMENTAL RESULTS

**Peptide Coating of QDs.** The modified protocol for  $\gamma$ PC coating is based on the previously published ampPC coating protocol,<sup>26,27</sup> but with some modifications. As before, the

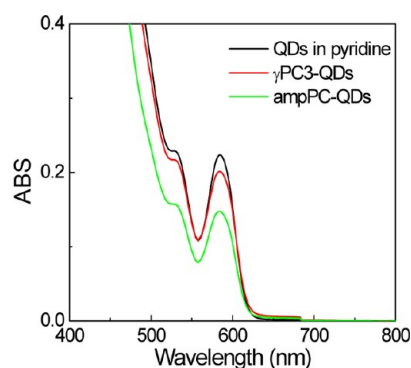
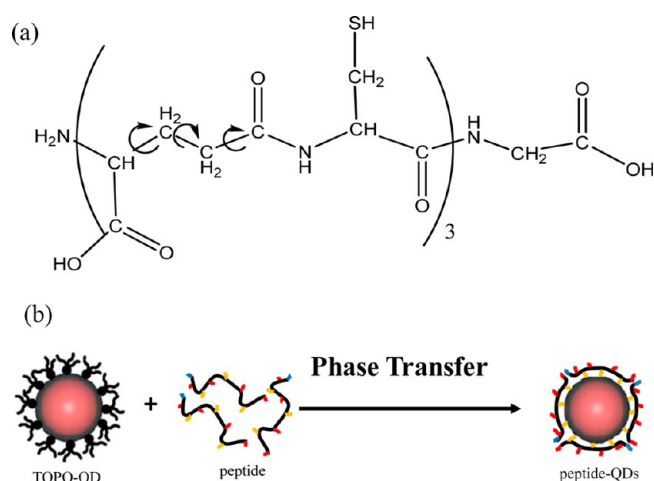


**Figure 1.** UV-vis absorption of QDs before peptide coating (black line) and after  $\gamma$ PC3 (red line) and ampPC (green line) coating. The absorptions represented the concentrations of the QDs and were used to compare the yield of coated QDs.

**Scheme 1.** (a) Structure of Phytochelatin Peptide ( $\gamma$ PC3) and (b) the Scheme for Surfactant Exchange with  $\gamma$ PC3 Peptides<sup>a</sup>



<sup>a</sup>The blue, red, and yellow bars in the chain represent amine, carboxylate, and thiol.

peptide coating exchange is based on displacing the original hydrophobic surfactants (e.g., trioctylphosphine oxide) with the cystinyl thiolates of the peptides. We introduced an intermediate step, constituting the dispersion of QDs in pyridine. Since the pyridine binds weakly to QDs surfaces, adding thiol contained peptides and adjusting the pH of the mixture to about pH 10 easily and quickly displaces the pyridines with the peptides. The gamma structure all-hydrophilic  $\gamma$ PCs were directly dissolved in water (in contrast to the amphiphilic ampPC, which were dissolved in organic solvents), and the subsequent ligand exchange reaction was performed in the aqueous solution. Therefore, the all-hydrophilic peptide and the modified protocol eliminated the extra (and wasteful) steps of dispersing QDs in DMSO, transferring them into water and reconcentrating them. The improvement in final product yield was demonstrated by comparing  $\gamma$ PC3 coated QDs with ampPC coated QDs that were prepared from identical starting materials (QDs in pyridine solution, of equal concentration and volume), diluted to the same 450  $\mu$ L volume. The final concentrations of both products were evaluated by comparing their UV-vis absorption spectra, as shown in Figure 1. The peak at 583 nm was the first absorption peak of QDs and corresponded to the concentration of QDs. By comparison, the absorption of the  $\gamma$ PC3 coated QDs was 90% of the original QDs in pyridine, whereas the absorption of ampPC coated QDs was only 67% of the starting material. The fewer steps not only reduced the preparation time and effort but also reduced the loss of sample during the water solubilization procedure.

**Colloidal Stability.** The  $\gamma$ -Glu containing peptide provides three additional carbons in between two adjacent Cys as compared to the  $\alpha$ -peptide (Scheme 1). These additional carbons provide greater degree of rotational freedom in the peptide backbone. We hypothesized that the added flexibility could facilitate better alignment of the thiols toward the metal ions on the QD's surface, resulting in better packing and therefore better colloidal stability for the particles. Colloidal stability was tested by a gel electrophoresis assay for QDs coated with Cys monomers, GSH monomers,  $\gamma$ PC3,  $\alpha$ PC3, and ampPC (Figure 2). All coated QDs formulations were purified through dialysis, and the concentration was adjusted to 1  $\mu$ M. Samples were stored at room temperature and under ambient

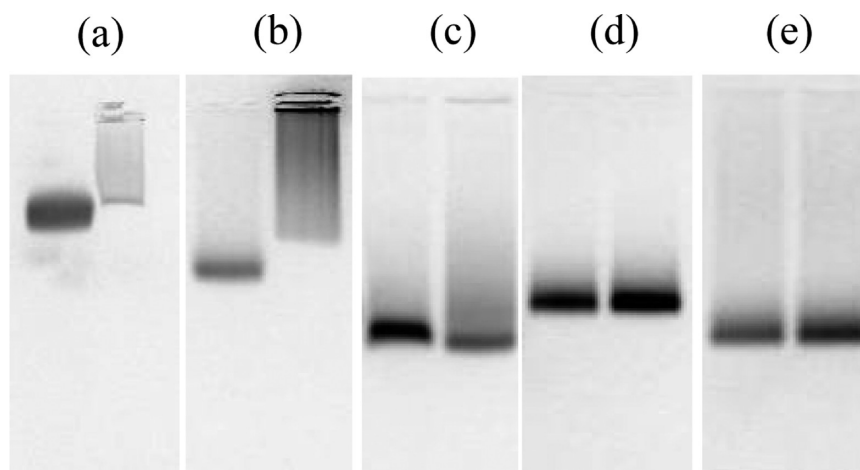


**Figure 2.** Gel electrophoresis of (a) Cys, (b) GSH, (c)  $\alpha$ PC3, (d)  $\gamma$ PC3, and (e) ampPC coated 602 nm emission QDs taken with a gel scanner; the dark bands represent QDs' fluorescence. The left lane of each gel image corresponds to freshly prepared QDs, the right lane corresponds to 1 day, 2 weeks, 1 month, 6 months, and 6 months room temperature stored QDs respectively.



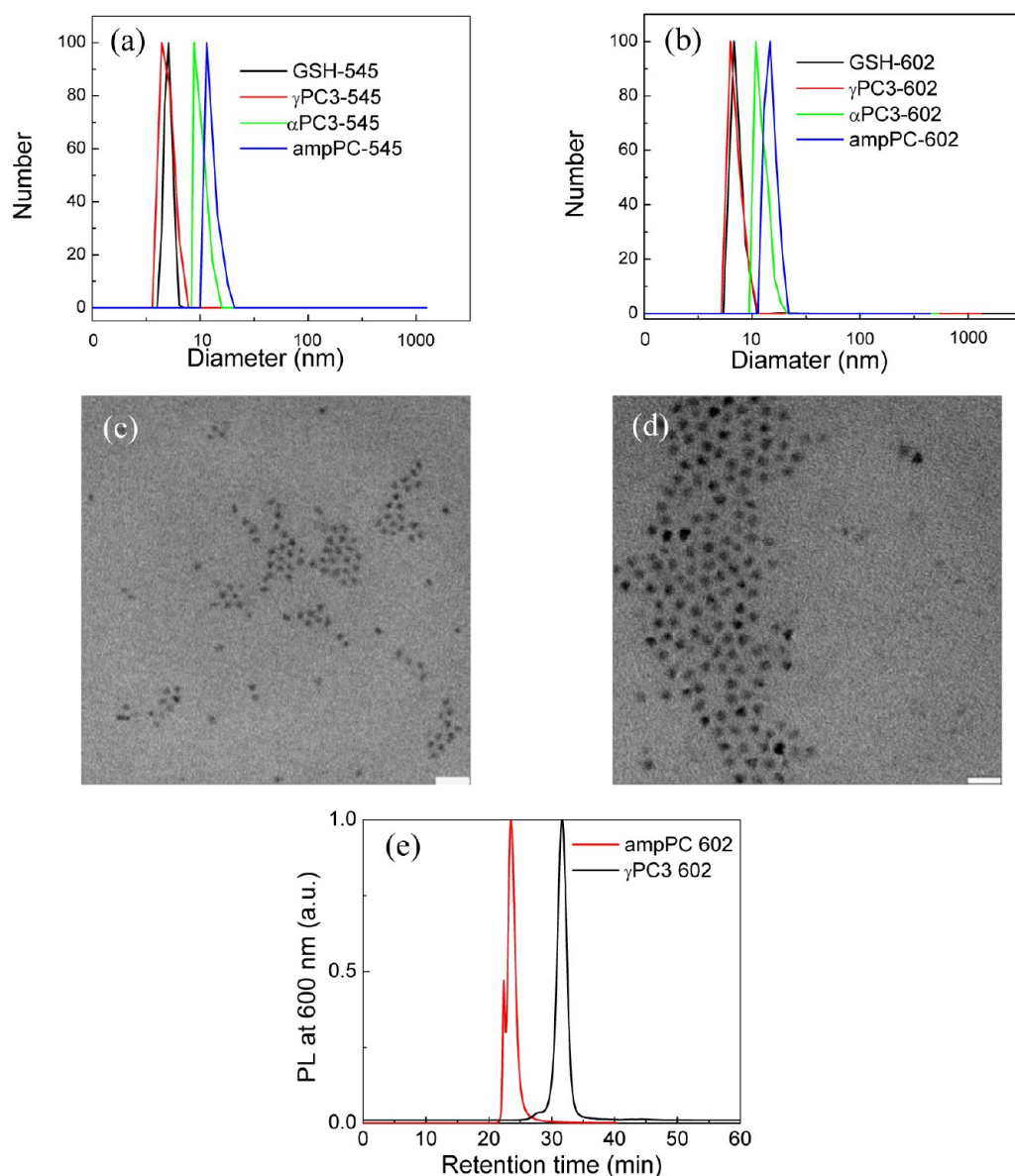


**Figure 3.** DLS measurements of coated QDs with various peptides for (a) 545 and (b) 602 nm emission QDs. Corresponding TEM images of (c) 545 and (d) 602 nm QDs (scale bar: 20 nm). Retention time of 602 nm QDs coated with ampPC or  $\gamma$ PC3 in a size exclusion column (e). Note the single, symmetric elution peak of the  $\gamma$ PC3 coating as compared to the ampPC peak.

room lighting. Due to the monothiol group and the photo-oxidation, the Cys and GSH coated 602 nm QDs precipitated out of solution after 1 day and 2 weeks, respectively, as judged by the smeared bands on the gel (a and b). GSH coated QDs remained stable in buffer longer than Cys coated QDs, indicating good binding affinity of GSH to the ZnS shell (consistent with previous reports<sup>31</sup>). We argue that a sequence containing multiple repeats of  $\gamma$ Glu-Cys should provide even stronger binding, due to higher avidity. A high colloidal stability of aged  $\gamma$ PC3 coated QDs (stored in buffer for 6 months) is indeed implied by a narrow band (d). In comparison, a 4 weeks old solution of QDs coated with the less flexible  $\alpha$ PC3 peptide (but having the same amino acid sequence and the same number of thiol groups) migrated in a smeared band (c). The ampPC peptide, with a larger number of thiol groups (6 cys), also exhibited good stability, as judged by its narrow band of 6 months aged solution (e). These results suggest that, although the increased number of thiols in a peptide increases its binding

affinity to the QD's surface, the flexibility of the chain also contributes to the improved colloidal stability (3 cysteine contained gamma structure coating showed better stability than 3 cysteine contained alpha structure coating did and was comparable to 6 cysteine contained alpha structure coating). One month aged  $\gamma$ PC3- and ampPC-coated QDs exhibited good stability also at pH 5 and 10 buffers (Supporting Information).

**Sizing of Peptide-Coated QDs.** Dynamic light scattering (DLS) and transmission electron microscopy (TEM) were utilized to assess the thickness of various coatings of the particles. Two inorganic CdSe/ZnS QDs diameters of  $3.5 \pm 0.5$  and  $5.3 \pm 0.8$  nm (as determined from TEM studies, Figure 3c,d) with respective emission peaks of 545 and 602 nm were used as reference points for these studies. The DLS results for the various coatings are shown in Figure 3a,b. The hydrodynamic diameters (HD) derived for GSH coating were  $5.1 \pm 1.3$  and  $6.9 \pm 1.8$  nm, respectively. The corresponding HDs for

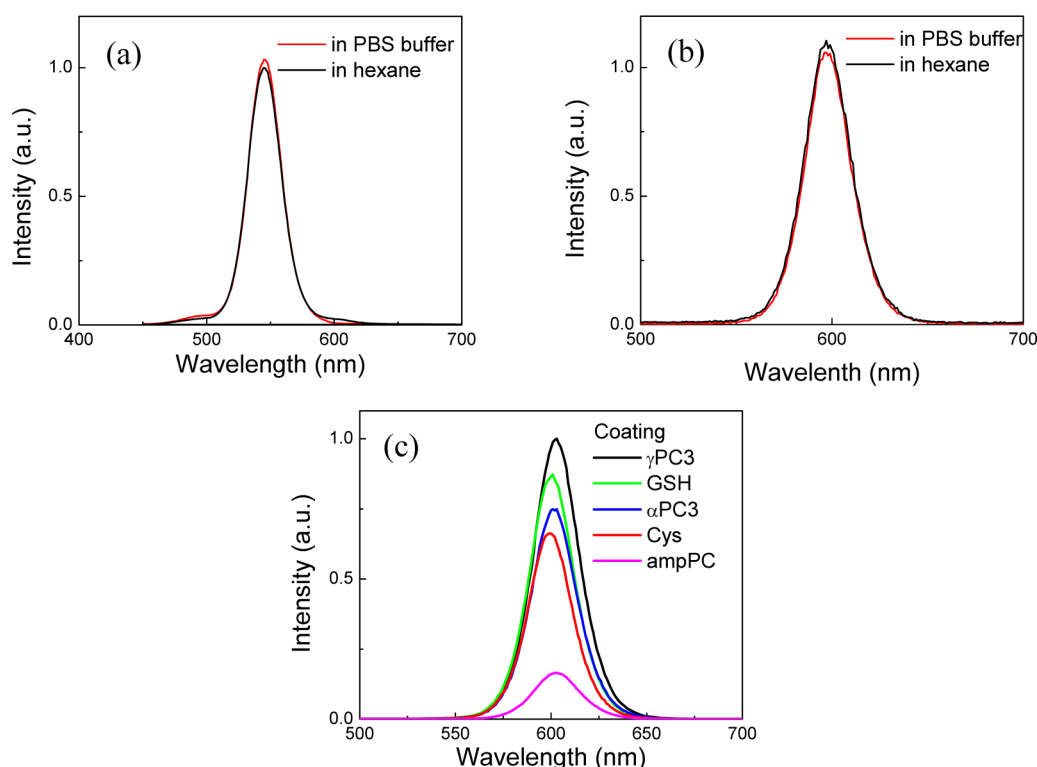


**Figure 4.** Fluorescence emission measurements of 545 (a) and 602 nm (b) of as-synthesized QDs and  $\gamma$ PC3-QDs. (c) Comparison of fluorescence emission at same concentration of various peptides coated 602 nm QDs.

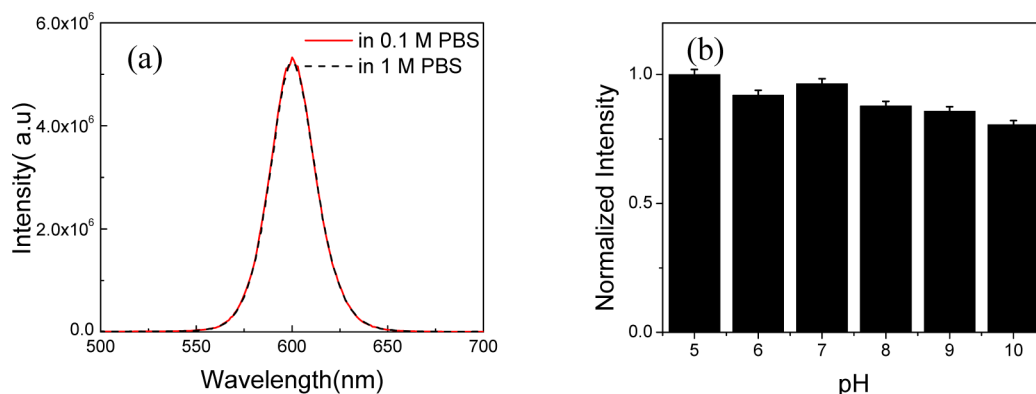


**Figure 5.** Effect of salt concentration (0.1 M sodium phosphate, 0.15 M sodium chloride and 1 M sodium phosphate, 1.5 M sodium chloride) (a) and pH (b) on fluorescence intensity of  $\gamma$ PC3-602 nm.

the  $\gamma$ PC3 coating were  $5.7 \pm 2.1$  and  $7.1 \pm 2.3$  nm (i.e., slightly larger than the monothiol GSH coating). These measurements show a  $\gamma$ PC3 coating thickness of  $\sim(1.6-1.8)/2 = 0.8-0.9$  nm. The corresponding HDs for the  $\alpha$ PC3 coating were  $9.6 \pm 2.4$  and  $12.6 \pm 3.2$  nm, implying a coating thickness of  $\sim(6.1-7.8)/2 = 3-3.9$  nm. This suggests that the  $\gamma$ PC3 peptide's orientation on the QD surface is different from that of the  $\alpha$ PC3 peptide (i.e.,  $\gamma$ PC3 is more tightly wrapped on the QD's surface due to its higher flexibility). The original ampPC coating<sup>27</sup> yielded HDs of  $12.0 \pm 4.0$  and  $14.1 \pm 4.5$  nm, respectively, implying a coating thickness of  $\sim(8.5-8.8)/2 = 4.2-4.4$  nm. In addition to the reduced size,  $\gamma$ PC3-QDs displayed more uniform sizes (narrower size distribution) as judged by size exclusion chromatography (Figure 3e).

**Relative Quantum Yield Measurements.** We hypothesize that the flexible structure of the  $\gamma$ PC3 peptide facilitates denser packing of thiol groups on the QD's surface and

therefore better elimination of charge traps on the surface. We argue that improved surface passivation should reduce quantum yield loss upon water solubilization. The relative fluorescence emission yields of the various coating formulations were therefore compared (using the same QDs concentration and volume). Figure 4 shows the fluorescence spectra of 545 (a) and 602 nm (b)  $\gamma$ PC3 coated CdSe/ZnS QDs before and after surfactant exchange. The fluorescence intensity of the  $\gamma$ PC3 coated particles in PBS buffer was only slightly decreased (or even slightly increased for the 545 nm QDs) as compared to that of the starting QDs material (in pyridine). On the basis of these relative fluorescence measurements, QYs were calculated to be  $52 \pm 1\%$  and  $47 \pm 1\%$  for 545 and 602 nm  $\gamma$ PC3-QDs, respectively (see the Supporting Information). We also compared fluorescence emissions of 602 nm QDs coated with Cys monomers, GSH monomers,  $\gamma$ PC3,  $\alpha$ PC3, and ampPC coatings in PBS buffer, yielding QYs of  $31 \pm 1\%$ ,  $41 \pm$

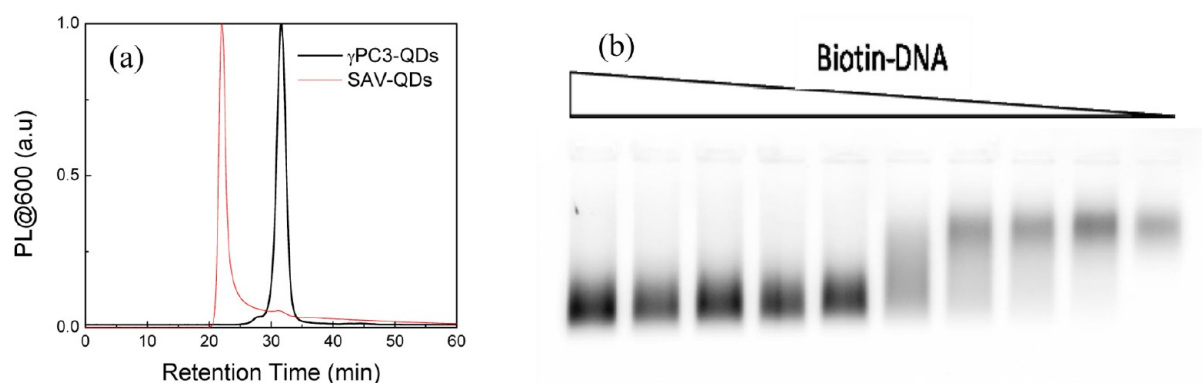


**Figure 6.** (a) Gel filtration chromatography (GFC) of SAV-QDs conjugates and  $\gamma$ PC3-QDs and (b) gel electrophoresis assay of biotinylated DNA bound to SAV-602 nm. The concentration ratio of biotinylated DNA to SAV-602 nm QDs was 200, 100, 50, 25, 12.5, 6.5, 3.25, 1.65, 0.85, and 0 from left to right.

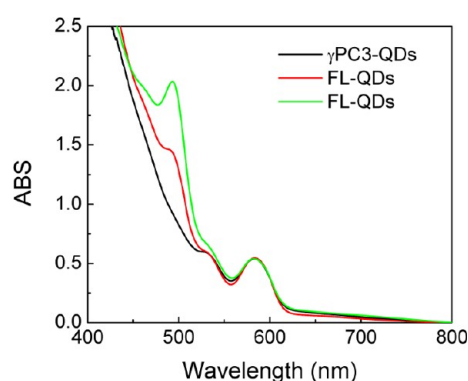


**Figure 7.** (a) UV-vis absorption of fluorescein (FL) coated QDs; the ratio of FL- $\gamma$ PC3 to PEG- $\gamma$ PC3 mixture is 0 (black line), 1:9 (red line), and 4:6 (green line).

1%,  $47 \pm 1\%$ ,  $36 \pm 1\%$ , and  $7 \pm 2\%$ , respectively. Lastly,  $\gamma$ PC3 602 nm QDs ( $QY = 47 \pm 1\%$ ) were used to study the effects of pH and salt concentration (Figure 5). No significant changes in QYs were observed for QDs in  $\times 1$  (0.1 M sodium phosphate, 0.15 M sodium chloride) and  $\times 10$  (1 M sodium phosphate, 1.5 M sodium chloride) PBS buffers, nor for QDs in pH buffer ranges between pH 5–10.

**Bioconjugation.** Peptide coating affords the introduction of carboxylic and amine reactive groups on the surface of the QDs, useful for further biofunctionalization. As an example, we conjugated streptavidin (SAV) to  $\gamma$ PC3 coated 602 nm QDs using bifunctional EDC linker chemistry.<sup>41</sup> Following the conjugation reaction, the  $\gamma$ PC3-QDs were purified (from excess SAV) and characterized using a gel filtration column, followed by an elution step using PBS buffer (Figure 6a, an elution peak for conjugated QDs at 22 min and an elution peak for unconjugated QDs at 31 min). The SAV-QDs conjugates were further purified (see the Supporting Information), incubated with different concentrations of 90 bp biotinylated ssDNA molecules (with concentration ratios of  $\times 200$ ,  $\times 100$ ,  $\times 50$ ,  $\times 25$ ,  $\times 12.5$ ,  $\times 6.5$ ,  $\times 3.25$ ,  $\times 1.65$ ,  $\times 0.85$ , and  $\times 0$ ) and analyzed by a gel shift assay ( $\times 200$  on the leftmost column and  $\times 0$  on the rightmost column). The fluorescent band smears-out for increasing ssDNA/SAV-QDs ratios (going from  $\times 0$  to  $\times 6.5$ , right-to-left). At ratios higher than  $\times 12.5$ , the gel shift forms a tight band, indicating saturation of all SAV binding sites.

We were also able to directly conjugate small molecules to  $\gamma$ PC3 peptides' amine groups in buffer before (and separate

from) QDs' surfactant exchange. Using this approach, we preconjugated fluorescein (FL) and polyethylene glycol (PEG) to  $\gamma$ PC3 (to form FL- $\gamma$ PC3 and PEG- $\gamma$ PC3). We could then control the number of fluoresceins per QD by tuning the molar ratio of the FL- $\gamma$ PC3/PEG- $\gamma$ PC3 mixture that was then used for surfactant exchange. The number of fluoresceins per single coated QD was estimated from UV-vis absorption<sup>27,40</sup> measurements, yielding four fluoresceins per single QD for 1:9 FL- $\gamma$ PC3/PEG- $\gamma$ PC3 mixture and seven fluoresceins per single QD for 4:6 FL- $\gamma$ PC3/PEG- $\gamma$ PC3 mixture (Figure 7).

**Live Cell Imaging.** To test targeting specificity of the resulted FL-QDs, we incubated the probes with N2A cells expressing the PrP prion protein, fused with a scFV against FL at the N terminus (extracellular side, scFv-PrP).<sup>40</sup> For control, FL-QDs were also incubated with wild type N2A. Panels a and c in Figure 8 are the bright field images of wild type and PrP-scFV expressed cells, respectively. Panels b and d in Figure 8 are the corresponding fluorescence images. As expected, only cells expressing the scFV-PrP protein were fluorescently stained (Figure 8d), whereas the nonexpressing cells hardly stained (Figure 8b).

**Small Animal Imaging.** To test the suitability of  $\gamma$ PC3-QDs for in vivo molecular imaging in small animals, we injected the probes into zebrafish and followed their biodistribution over time by time-lapse microscopy. Zebrafish was chosen as a model animal system due to its optical transparency, rapid development, susceptibility to genetic manipulation, and mammalian-like vasculature. 1  $\mu$ M  $\gamma$ PC3 602 nm QDs in buffer were injected into the zebrafish heart at 3 day post fertilization (dpf) using 2–3 injection pulses and observed under a fluorescence microscope. As clearly shown in Figure 9a,  $\gamma$ PC3 602 nm QDs were homogeneously dispersed into the blood vasculature immediately after injection, lighting up the entire vascular network. In particular, the trunk vasculature and the repetitive pattern of dorsoventral intersegmental vessels were distinctively visualized. However, the probes were found to gradually accumulate over time along the bottom trunk (along the tail, Figure 9b). This accumulation could be possibly related to phagocytosis by reticular cells and secretion out of the body,<sup>42</sup> as evident by disappearance of fluorescence by three days after injection (Figure 9c,d). We also note that the mortality of QDs injected embryos and/or mal-development were very small (two out of sixty fishes died afterward) which is similar to that of uninjected embryos.

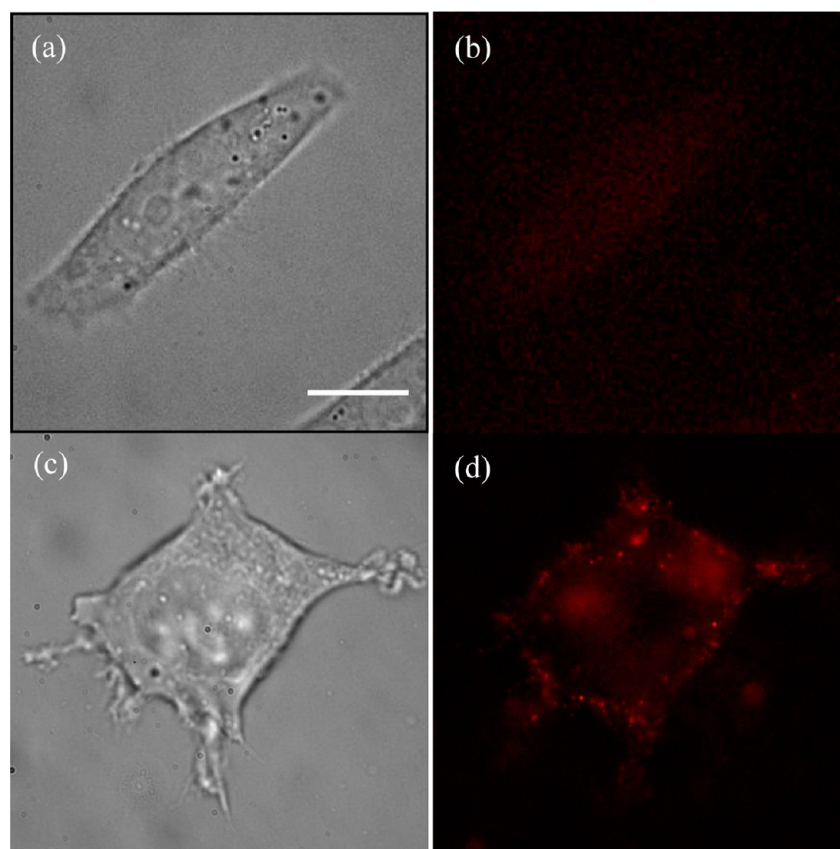


**Figure 8.** FL-QDs labeling of live N2A cells without (a and b) and with (c and d) expression of scFV-PrP on the plasma membrane showing specificity for FL-QDs; (a and c) bright filed; (b and d) fluorescence images; scale bar: 4  $\mu\text{m}$ .

## DISCUSSION

We have demonstrated that water solubilization of QDs with  $\gamma\text{PC3}$  is as effective as water solubilization with ampPC but with a the following added benefits: (i) elimination of the (wasteful) QDs' dispersion in DMSO step; (ii) higher recovery of final (water-soluble) product; (iii) smaller diameter of final product; (iv) higher QY in water (as compared to ampPC coat); (v) facile bioconjugation either through carboxylic or through amine reactive groups. At the same time, the  $\gamma\text{PC3}$  coating maintains the advantage of the ampPC coating, including: (vi) excellent colloidal stability and long shelf-lifetime; (vii) minimal nonspecific binding and good specific targeting; and (viii) good in vivo biodistribution. We emphasize that attributes iii–viii are maintained at the same time.

Taken together, the experimental observations described above suggest that hydrophobic amino acids are not required for the correct orientation of cysteines' thiol groups toward the surface of the QD.<sup>26,27</sup> On the contrary, the higher flexibility of  $\gamma\text{PC3}$  seems to provide better surface coverage and therefore better surface passivation. Moreover, the observed variations in relative QYs are likely due to the degree of surface passivation achieved by the various coats. The high QY attained for GSH and  $\gamma\text{PC3}$  coats is consistent with previous reports<sup>37</sup> and is likely due to their tight binding to CdS and ZnS surfaces. The multidentate nature of  $\gamma\text{PC3}$  and  $\alpha\text{PC3}$  could explain the higher QY as compared to GSH and Cys, respectively. As previously reported, ampPC coating yielded a QY of only  $7 \pm 2\%$ .<sup>27,29</sup> Presumably, the relatively long and stiff ampPC does not uniformly saturate all dangling bonds on the QDs' surface. We previously reported an increase in ampPC coated QDs'

QYs upon UV illumination<sup>29</sup> and more recently found that adding small thiolated molecule like DTT during the ampPC coating process increased their QYs (data not shown). Others have also reported a slight increase in QYs of GSH coated QDs over a period of 2–3 days after preparation.<sup>38</sup> These observations suggest that full saturation of all dangling bonds and/or surface reconstruction are required for achieving high QYs in buffer. The good photophysical properties of  $\gamma\text{PC3}$ -QDs in different (salt and pH) environments also attest to the enhanced stability of this improved coating.

Lastly, it is interesting to note that protein conjugation to thiol ligands-coated QDs (such as DHLA) by EDC chemistry is difficult,<sup>12</sup> possibly because of the very facile reaction between the carbodiimide and the thiol (Carraway and Triplett reported that EDC reacts with mercaptoethanol with a pseudofirst-order rate constant of  $0.029 \text{ s}^{-1}$  for 0.1 M EDC, 0.013 M mercaptoethanol, 25  $^{\circ}\text{C}$ , pH 5.0<sup>43</sup>). When we introduced a 3000 fold excess of EDC to activate the carboxylic groups on the QDs surface, the Cys monomers, GSH monomers,  $\alpha\text{PC3}$ , and ampPC coated QDs precipitated and/or lost fluorescence during the reaction, whereas  $\gamma\text{PC3}$  coated QDs maintained good colloidal dispersion and high QY and were successfully conjugated to SAV. These findings support the notion that  $\gamma\text{PC3}$  binds very strongly to the QD's surface and cannot be removed by a large excess of EDC.

## CONCLUSION

We demonstrated a flexible, gamma structure, cysteine-rich, all hydrophilic peptide sequence (phytochelatin peptide) and an efficient protocol to coat QDs with such a peptide. These



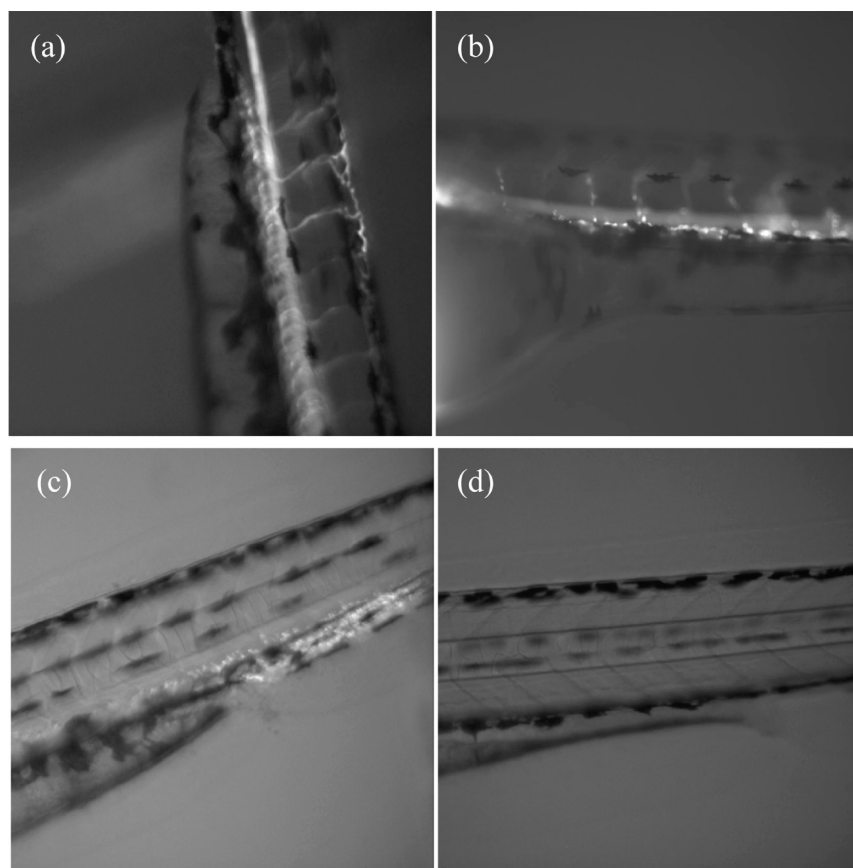


**Figure 9.** Images of zebrafish injected with  $\gamma$ PC3 coated 602 nm QDs at different intervals post injections (a) 10 min, (b) 1 h, (c) 1 days, and (d) 3 days.

coated QDs displayed superior colloidal stability (over a large range of salt concentrations and pH), small size due to the thin coating (0.8–0.9 nm), and high QY (comparable to organic phase QDs and older generation peptide-coated QDs). Our results suggest that the more flexible gamma structure peptide affords a favorable orientation and binding of thiol groups to the QDs surface. In addition, this novel peptide coat offers versatile and facile for bioconjugation approaches. We demonstrated live cell imaging and in vivo zebrafish imaging with these optimized QDs. The new coating simultaneously provides good colloidal stability, compact size, high QY, easy functionalization, and good biocompatibility.

## ■ ASSOCIATED CONTENT

### ● Supporting Information

Mass spectrum and HPLC characterization of synthetic peptide, QY measurements, and UV–vis spectra monitoring SAV-602 nm purification are available as Supporting Information. This material is available free of charge via the Internet at <http://pubs.acs.org>.

## ■ AUTHOR INFORMATION

### Corresponding Author

\*E-mail: [sweiss@chem.ucla.edu](mailto:sweiss@chem.ucla.edu). Phone: 310-794-0093.

### Notes

The authors declare no competing financial interest.

## ■ ACKNOWLEDGMENTS

We thank Laurent Bentolila for helping with zebrafish injections. We also thank Catalina Marambio and Eric Hoek for the assistance in dynamic light scattering experiments. This work was supported by NIH Grant No. 5R01EB000312 and NIH Grant No. 1R01GM086197. Fluorescent imaging was done at the CNSI Advanced Light Microscopy/Spectroscopy Shared Facility at UCLA. TEM images were taken at the CNSI Electron Imaging Center at UCLA.

## ■ REFERENCES

- (1) Pinaud, F.; Michalet, X.; Bentolila, L. A.; Tsay, J. M.; Doose, S.; Li, J. J.; Iyer, G.; Weiss, S. *Biomaterials* **2006**, *27*, 1679–1687.
- (2) Alivisatos, P. *Nat. Biotechnol.* **2004**, *22*, 47–52.
- (3) Medintz, I. L.; Mattoussi, H.; Clapp, A. R. *Int. J. Nanomed.* **2008**, *3*, 151–167.
- (4) Michalet, X.; Pinaud, F. F.; Bentolila, L. A.; Tsay, J. M.; Doose, S.; Li, J. J.; Sundaresan, G.; Wu, A. M.; Gambhir, S. S.; Weiss, S. *Science* **2005**, *307*, 538–544.
- (5) Li, J. J.; Wang, Y. A.; Guo, W.; Keay, J. C.; Mishima, T. D.; Johnson, M. B.; Peng, X. *J. Am. Chem. Soc.* **2003**, *125*, 12567–12575.
- (6) Peng, Z. A.; Peng, X. *J. Am. Chem. Soc.* **2001**, *123*, 183–184.
- (7) Talapin, D. V.; Rogach, A. L.; Kornowski, A.; Haase, M.; Weller, H. *Nano Lett.* **2001**, *1*, 207–211.
- (8) Gao, X.; Cui, Y.; Levenson, R. M.; Chung, L. W.; Nie, S. *Nat. Biotechnol.* **2004**, *22*, 969–976.
- (9) Yu, W. W.; Chang, E.; Falkner, J. C.; Zhang, J.; Al-Somali, A. M.; Sayes, C. M.; Johns, J.; Drezek, R.; Colvin, V. L. *J. Am. Chem. Soc.* **2007**, *129*, 2871–2879.
- (10) Dubertret, B.; Skourides, P.; Norris, D. J.; Noireaux, V.; Brivanlou, A. H.; Libchaber, A. *Science* **2002**, *298*, 1759–1762.



- (11) Chan, W. C. W.; Nie, S. *Science* **1998**, *281*, 2016.
- (12) Mattoussi, H.; Mauro, J. M.; Goldman, E. R.; Anderson, G. P.; Sundar, V. C.; Mikulec, F. V.; Bawendi, M. G. *J. Am. Chem. Soc.* **2000**, *122*, 12142–12150.
- (13) Pathak, S.; Choi, S. K.; Arnheim, N.; Thompson, M. E. *J. Am. Chem. Soc.* **2001**, *123*, 4103–4104.
- (14) Pons, T.; Mattoussi, H. *Ann. Biomed. Eng.* **2009**, *37*, 1934–1959.
- (15) Smith, A. M.; Nie, S. *J. Am. Chem. Soc.* **2008**, *130*, 11278–11279.
- (16) Liu, W.; Choi, H. S.; Zimmer, J. P.; Tanaka, E.; Frangioni, J. V.; Bawendi, M. *J. Am. Chem. Soc.* **2007**, *129*, 14530–14531.
- (17) Choi, H. S.; Liu, W.; Misra, P.; Tanaka, E.; Zimmer, J. P.; Itty Ipe, B.; Bawendi, M. G.; Frangioni, J. V. *Nat. Biotechnol.* **2007**, *25*, 1165–1170.
- (18) Chan, W. C. W.; Maxwell, D. J.; Gao, X. H.; Bailey, R. E.; Han, M. Y.; Nie, S. M. *Curr. Opin. Biotechnol.* **2002**, *13*, 40–46.
- (19) Mei, B. C.; Susumu, K.; Medintz, I. L.; Delehanty, J. B.; Mountziaris, T. J.; Mattoussi, H. *J. Mater. Chem.* **2008**, *18*, 4949–4958.
- (20) Uyeda, H. T.; Medintz, I. L.; Jaiswal, J. K.; Simon, S. M.; Mattoussi, H. *J. Am. Chem. Soc.* **2005**, *127*, 3870–3878.
- (21) Liu, W.; Howarth, M.; Greytak, A. B.; Zheng, Y.; Nocera, D. G.; Ting, A. Y.; Bawendi, M. G. *J. Am. Chem. Soc.* **2008**, *130*, 1274–1284.
- (22) Susumu, K.; Mei, B. C.; Mattoussi, H. *Nat. Protoc.* **2009**, *4*, 424–436.
- (23) Susumu, K.; Uyeda, H. T.; Medintz, I. L.; Pons, T.; Delehanty, J. B.; Mattoussi, H. *J. Am. Chem. Soc.* **2007**, *129*, 13987–13996.
- (24) Liu, W. H.; Greytak, A. B.; Lee, J.; Wong, C. R.; Park, J.; Marshall, L. F.; Jiang, W.; Curtin, P. N.; Ting, A. Y.; Nocera, D. G.; et al. *J. Am. Chem. Soc.* **2010**, *132*, 472–483.
- (25) Iyer, G.; Pinaud, F.; Tsay, J.; Li, J. J.; Bentolila, L. A.; Michalet, X.; Weiss, S. *IEEE Trans. Nanobiosci.* **2006**, *5*, 231–238.
- (26) Iyer, G.; Pinaud, F.; Tsay, J.; Weiss, S. *Small* **2007**, *3*, 793–798.
- (27) Pinaud, F.; King, D.; Moore, H. P.; Weiss, S. *J. Am. Chem. Soc.* **2004**, *126*, 6115–6123.
- (28) Tsay, J. M.; Doose, S.; Weiss, S. *J. Am. Chem. Soc.* **2006**, *128*, 1639–1647.
- (29) Tsay, J. M.; Doose, S.; Pinaud, F.; Weiss, S. *J. Phys. Chem. B* **2005**, *109*, 1669–1674.
- (30) Cobbett, C. S. *J. Biol. Chem.* **2001**, *276*, 183–188.
- (31) Bae, W. O.; Abdullah, R.; Henderson, D.; Mehra, R. K. *Biochem. Biophys. Res. Commun.* **1997**, *237*, 16–23.
- (32) Spreitzer, G.; Whitling, J. M.; Madura, J. D.; Wright, D. W. *Chem. Commun.* **2000**, 209–210.
- (33) Whitling, J. M.; Spreitzer, G.; Wright, D. W. *Adv. Mater.* **2000**, *12*, 1377–1380.
- (34) Zheng, Y.; Gao, S.; Ying, J. *Adv. Mater.* **2007**, *19*, 376–380.
- (35) Zheng, Y.; Yang, Z.; Ying, J. *Adv. Mater.* **2007**, *19*, 1475–1479.
- (36) Baumle, M.; Stamou, D.; Segura, J. M.; Hovius, R.; Vogel, H. *Langmuir* **2004**, *20*, 3828–3831.
- (37) Zheng, Y.; Yang, Z.; Li, Y.; Ying, J. *Adv. Mater.* **2008**, *20*, 3410–3415.
- (38) Jin, T.; Fujii, F.; Komai, Y.; Seki, J.; Seiyama, A.; Yoshioka, Y. *Int. J. Mol. Sci.* **2008**, *9*, 2044–2061.
- (39) Boder, E. T.; Midelfort, K. S.; Wittrup, K. D. *Proc. Natl. Acad. Sci. U.S.A.* **2000**, *97*, 10701–10705.
- (40) Iyer, G.; Michalet, X.; Chang, Y.; Pinaud, F.; Matyas, S.; Payne, G.; Weiss, S. *Nano Lett.* **2008**, *8*, 4618–4623.
- (41) Grabarek, Z.; Gergely, J. *Anal. Biochem.* **1990**, *185*, 131–135.
- (42) Rieger, S.; Kulkarni, R. P.; Darcy, D.; Fraser, S. E.; Koster, R. W. *Dev. Dyn.* **2005**, *234*, 670–681.
- (43) Carraway, K. L.; Triplett, R. B. *Biochim. Biophys. Acta* **1970**, *200*, 564–566.